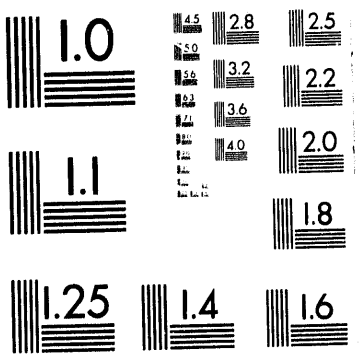
1.0
1.1
1.25
1.4
1.6
1.8
2.0
2.2
2.5
2.8
3.2
3.6
4.0
4.5
5.0
5.6

1 of 1

DOE/MC/30097-3516
(DE94000046)

Air Quality Assessment and Control
Task 2.0

Semi-Annual Report
March 1 - June 30, 1993

S.J. Miller
D.L. Laudal
M.K. Heidt

July 1993

Work Performed Under Cooperative Agreement No.: DE-FC21-93MC30097

For
U.S. Department of Energy
Office of Fossil Energy
Morgantown Energy Technology Center
Morgantown, West Virginia

By
Energy & Environmental Research Center
University of North Dakota
Grand Forks, North Dakota

DISCLAIMER

This cover stock is 30% post-consumer waste
and 30% pre-consumer waste, and is recyclable.

DOE/MC/30097-3516
(DE94000046)
Distribution Category UC-107

Air Quality Assessment and Control
Task 2.0

Semi-Annual Report
March 1 - June 30, 1993

S.J. Miller
D.L. Laudal
M.K. Heidt

Work Performed Under Cooperative Agreement No.: DE-FC21-93MC30097

For
U.S. Department of Energy
Office of Fossil Energy
Morgantown Energy Technology Center
P.O. Box 880
Morgantown, West Virginia 26507-0880

By
Energy & Environmental Research Center
University of North Dakota
15 North 23rd Street
Grand Forks, North Dakota 58203

July 1993

TABLE OF CONTENTS

LIST OF FIGURES

LIST OF FIGURES (continued)

EXECUTIVE SUMMARY

Emissions of fine particles are of concern because these particles can be deposited in the lower respiratory system through normal breathing. The potential problem is further compounded because hazardous trace elements, such as selenium and arsenic, are known to be concentrated on such fine particles. Control device removal efficiency is lowest for respirable particles, so the potentially most hazardous particles from coal combustion are collected with the lowest removal efficiency. The 1990 Clean Air Act Amendments address the issue of emissions of acid rain precursors, require the study of air toxic emissions, and provide for possible expansion of visibility protection measures. Therefore, a current need exists to develop superior, but economical, methods to control emissions of air toxic particulate matter. One approach is to model the relationships between the cohesive properties of fly ash and particulate collector performance in electrostatic precipitators (ESPs) and fabric filters. In ESPs, a balance between good dust release and minimum redispersion must be achieved for optimum ESP fine-particle collection efficiency. To achieve high fine-particle collection efficiency with fabric filters, the large pores in the fabric must be adequately bridged, and reentrainment must be kept to a minimum while still allowing for adequate dust cake release. However, the defining relationships between cohesive dust properties and particulate collector performance have not been adequately developed.

Therefore, the goal of the Fine Particulate Control project is the development of methods to measure the cohesive strength and reentrainment potential of fly ashes and to model emissions of fine particles based on these measurements. A long-term project goal is to develop the models to the point where they can be used to help design particulate control devices for the lowest level of fine-particle emissions at a reasonable cost.

Recent results show that tensile strength, aerated porosity, and packed porosity measurements are appropriate methods to quantify the cohesive properties of fly ash. Fly ashes with tensile strengths of less than 50 N/m^2 are likely to have significantly greater ESP rapping dispersion of fine particles than fly ashes with tensile strengths greater than 250 N/m^2. Fly ash tensile strength also appears to be a good predictor of fabric filter particulate emissions. Fine-particle emissions from a pulse-jet baghouse with Ryton felted fabric were 100 times greater for a fly ash with a tensile strength less than 100 N/m^2 compared to fly ashes with tensile strengths greater than 250 N/m^2. In direct pore-bridging experiments with monosized openings, tensile strength was found to be an indicator of maximum bridging velocity. In tests with pulse jet-cleaned Ryton bags, packed porosity was a good indicator of initial or effective K_2. Bench-scale tests, however, indicate that particle size and face velocity must also be incorporated into a model to predict pressure drop as a function of dust properties. Reentrainment tests indicate that velocity is one of the most important parameters affecting pore-bridging ability and whether reentrainment will occur. Future efforts will attempt to incorporate particle size and velocity into a more general model.

TASK 2.0 AIR QUALITY ASSESSMENT AND CONTROL

Subtask 2.2 Fine-Particulate Control

Introduction

The Air Quality Assessment and Control project category consists of three tasks as presented in the Annual Project Plan:

Task 2.1: Air Toxics
Task 2.2: Fine-Particulate Control
Task 2.3: Novel Flue Gas-Cleaning Methods

Only Task 2.2, Fine-Particulate Control, is currently funded, and research activities for the project this reporting period have been entirely in support of Task 2.2. Therefore, the semiannual report for this project summarizes work in the fine particulate control area only.

- BACKGROUND

Emissions of fine particles are of concern because these particles can be deposited in the lower respiratory system through normal breathing. The potential problem is further compounded because hazardous trace elements, such as selenium and arsenic, are known to be concentrated on such fine particles. Control device removal efficiency is lowest for respirable particles, so the potentially most hazardous particles from coal combustion are collected with the lowest removal efficiency. In addition to potentially causing adverse health effects, fine particles, including secondary sulfates, are the primary cause of visibility impairment in the atmosphere. The 1990 Clean Air Act Amendments address the issue of emissions of acid rain precursors, require the study of air toxic emissions, and provide for possible expansion of visibility protection measures. Therefore, a current need exists to develop superior, but economical, methods to control emissions of SO_2, NO_x, and air toxic particulate matter.

Previous research at the Energy & Environmental Research Center (EERC) has focused on two areas: 1) bench-scale efforts to investigate the relationships between fine-particle emissions from fabric filters or electrostatic precipitators (ESPs) and the cohesive properties of fly ash and 2) investigation of the impact of coal combustion on atmospheric visibility. Control of fine-particle emissions from coal-fired boilers is an issue because of the current concern over air toxics in the atmosphere, which contain high concentrations of trace elements. The best method of minimizing the emission of these air toxic trace elements to the atmosphere is to install high-efficiency fine-particle control devices. Previous research has shown that the collectibility of fine-particles from coal combustion is highly dependent on the cohesive properties of the fly ash. Therefore, past research has focused on quantitative measurements of cohesive properties of fly ash and filtration behavior. The goal is to achieve the lowest level of fine-particle emissions, without an economic penalty, either by modifying the ash properties or by other design optimization methods. Significant progress has already been made toward this goal, but further bench-scale work is needed to develop and test models that predict fine-particle emissions based on ash properties.

Objectives

The goal of Task 2.2 is the development of methods to measure the cohesive strength and reentrainment potential of fly ashes and to model emissions of fine particles based on these measurements. Past research has concentrated on development of reliable methods to measure the cohesive properties of fly ash. While further refinement of these methods is desirable, they are already developed to the point where they can be used for modeling efforts. Therefore, the primary goal of the fine-particulate control task for the current project year is to develop a model that relates cohesive properties to fine-particle emissions and one that relates cohesive properties to flow resistance. The primary elements of the models will include tensile strength, porosity, particle size, pore-bridging ability (or, conversely, reentrainment potential), and face velocity. A long-term project goal is to develop the models to the point where they can be used to help design particulate control devices for the lowest level of fine-particle emissions at a reasonable cost.

● PLANNED WORK

The planned work, as stated in the Annual Research Plan, consists primarily of bench-scale experiments to measure the cohesive properties of fly ash samples and bench-scale pore-bridging/reentrainment tests. Procedures have already been developed from previous work, but tests have been completed with only a limited number of ash samples. Preliminary review of existing data indicates that the pore-bridging ability of a dust can be predicted by cohesive measurements such as tensile strength. However, the relationship needs to be verified with more data. Similarly, existing data indicate that the flow resistance of a dust can be predicted from cohesive measurements such as the aerated or packed porosity. However, results also show that both particle size and face velocity must be incorporated into the model to accurately predict the flow resistance from measured dust characteristics.

The fly ash samples for testing this project year were to be selected from our stored fly ash sample inventory, based on previous fabric filtration experiments at the EERC. The planned cohesive measurements consist primarily of tensile strength measurements, conducted with a Cohetester, and aerated or packed porosity measurements, conducted with a powder characteristics tester. The planned pore-bridging/reentrainment tests consist of filtration tests with precision metal electroformed sieves of exact pore dimensions. The dust for these tests is dispersed with a dry powder disperser, and particulate emissions are measured downstream of the filter with a laser particle sizer. Visual observation of the clean and dirty sides of the screens provides information on the conditions when complete pore bridging occurs or when reentrainment occurs. The new data will then be combined with the existing data to provide the information necessary for model development. The model will attempt to predict fine-particle collection efficiency and pressure drop as a function of fly ash tensile strength, aerated and/or packed porosity, particle size, pore-bridging ability (or, conversely, reentrainment potential), and face velocity. Other possible model inputs include chemical composition, particle morphology, and specific surface area. Model development will follow a logical progression, starting with the parameters that are known to have major effects, and then progressing with inputs from the minor effects. Parallel to the experimental work will be an ongoing evaluation of pertinent literature to aid in the modeling efforts.

Accomplishments

Work for this reporting period is divided into three activities:

- Preliminary modeling efforts to relate cohesive measurements to particulate collector performance
- Measurement of cohesive properties of additional fly ash samples
- Bench-scale pore-bridging and reentrainment experiments

● PRELIMINARY MODELING EFFORTS

Recent concern about fine-particle air toxic emissions has generated renewed interest in economical methods to improve fine-particle collection efficiency of both ESPs and baghouses. One approach is to model the relationships between the cohesive properties of fly ash and particulate collector performance. Cohesive properties of fly ash have been known for many years to influence the collectibility of fly ash in ESPs. White (1) devotes a whole chapter in his book to reentrainment effects in ESPs, but does not identify a specific dust characteristic that influences the level of reentrainment. Dismukes (2) identifies a change in fly ash cohesiveness as one of the mechanisms by which conditioning agents improve ESP performance, but does not present any quantitative data on the cohesive properties of fly ash. Spencer (3) identifies fly ash tensile strength as an important consideration in the study of ESP rapping, but does not relate tensile strength to any specific performance data. Particle adhesion was recognized by Billings and Wilder as an important parameter affecting fabric cleanability (4) and Dennis and coworkers stress that cohesive fly ash properties are important to fabric filter performance, but they were not incorporated into their filtration model (5). More recently, Bush and coworkers (6) have identified cohesivity as the primary ash characteristic affecting baghouse pressure drop and have presented effective angle of internal friction and compacted porosity as quantitative laboratory measurements of cohesive fly ash characteristics. Bush and coworkers correlate effective angle of internal friction and compacted porosity with residual dust cake weight for a narrow data set of baghouses with reverse-gas cleaning and woven-glass fabric. No attempt was made to correlate particulate emissions with cohesive characteristics. We have previously emphasized the importance of cohesive dust properties in the study of how conditioning can be applied to fabric filters to improve performance (7, 8). However, the defining relationships between cohesive dust properties and particulate collector performance have not been adequately developed.

In ESPs, an ideal dust would readily release from the plates upon rapping and fall to the hopper with minimum redispersion. Cake release, rapping reentrainment, and hopper reentrainment are all likely to be impacted by the cohesive properties of the dust. To achieve good dust cake release, a minimum cohesive or tensile strength would appear desirable, but to minimize redispersion of the dust into its original particle-size distribution, high dust tensile strength is preferred. Since these two factors are in direct opposition, a balance between good dust release and minimum redispersion must be achieved for optimum ESP performance.

Fabric filter performance is also impacted by cohesive dust properties. Since most fabrics have significantly larger pore sizes than the median particle size of the collected dust, high particle collection efficiency cannot occur unless the pores are effectively bridged. If pores are not adequately bridged, high-velocity pinholes can develop in the dust cake, leading to poor collection efficiency. Ideally, starting with a new fabric, the large pores should be bridged in the first filtration cycle and then remain bridged when the bags are cleaned. If emissions spikes occur after bag cleaning when many of the larger pores are opened, the pores must be bridged over again during each cleaning cycle to maintain a high collection efficiency. To achieve good pore bridging in fabric filters, high cohesive strength would appear to be desirable.

Independent of the pore-bridging ability of the dust is the cake-release character of the dust cake. The cake should release from the fabric with minimum energy input, without significant redispersion of the dust, while maintaining some minimum residual dust cake to help achieve a high collection efficiency. The relationship between cohesive dust properties and collection efficiency in a fabric filter is analogous to that in an ESP. In both cases, the dust must be low enough in cohesive strength to release readily, but high enough in cohesive strength to minimize reentrainment. However, with fabric filters the impact of cohesive dust characteristics on performance is more complex, because the cohesive properties are also likely to have a major effect on pressure drop. Besides particle-size effects, the primary cake properties that determine pressure drop are the cake porosity and thickness. Low cohesive strength appears to facilitate good cake release and low residual dust cake thickness, while high cohesive strength seems necessary to maintain a high dust cake porosity and prevent significant dust cake packing. Obviously, there must be a proper balance between these factors to optimize both particulate collection efficiency and pressure drop in fabric filters.

The cohesive properties of fly ash are important to the optimization of ESP and fabric filter performance. However, cohesive strength, along with other similar terms such as cohesivity and cohesiveness, is not well defined. Therefore, the first step to optimize collector performance is to select key cohesive characteristics that are well defined and can be quantitatively measured. Tensile strength and aerated or packed porosity are two such quantitative measurements. We have previously presented extensive data on the tensile strength and porosity of fly ash and here present initial correlations between these properties and control device performance.

– Measurement of Cohesive Fly Ash Properties

Previous attempts to quantitatively measure cohesive properties of powders included the Jenike flow-factor tester and a tilting table apparatus. Several shear methods have also been used to measure the flow properties of bulk solids. One shear method is the rotational ring shear device, which Southern Research Institute has used to measure cohesive properties of fly ash (9). From the ring shear data, the effective angle of internal friction was selected as the most useful parameter, with typical values ranging from 31° to 47° for coal fly ash. One apparent disadvantage of the ring shear method, however, is that the porosity of the shear layer is generally not known. More recently, Pontius reported that an electrostatic tensiometer can measure the tensile strength of powders by exposing a sample of the powder to an electrostatic field generated in a parallel-plate electrode system (10). Tensiometer-determined tensile strengths for powders, including fly

ash in the range of 1 to 15 N/m^2, appear to be somewhat lower than fly ash tensile strengths reported for other methods.

Initial development of an instrument to directly and quantitatively measure the tensile strength of powders occurred in the early 1960s at Warren Spring Laboratory in England (11). In the Warren Spring Laboratory apparatus, a powder sample was compacted under a controlled normal load into a cylindrical cell that was split diametrically. This apparatus served as the basis for the development of a commercially available instrument, called a Cohetester, which directly measures the tensile strength of bulk powders as a function of compaction pressure and is commercially available from Hosokawa Micron International, Inc. Yokoyama reported tensile strengths for bulk powders in the range of 18 to 440 N/m^2 in developmental research for the Cohetester (12). Since we have previously presented extensive data obtained at the EERC with the Cohetester, no further discussion on the Cohetester is given here (13, 14).

Since dust cake porosity will have a major effect on baghouse pressure drop, a direct determination of fly ash porosity in the laboratory would appear to be a relevant measurement. ASTM standard test methods for determination of the tap density of refractory metal powders (B527) and for determination of tapped packing density of catalyst particles (D4164) are possible measurements that could be applied to fly ash. Both methods are straightforward in that a bulk sample is placed in a glass graduated cylinder, which is tapped either 1000 (D4164) or 3000 (B527) times. The volume after tapping and sample weight provide the information to calculate the tapped density. Quantachrome Corporation manufactures an instrument called the Dual Autotap which conforms to ASTM standard test procedures B527 and D4164. These ASTM methods have not been applied to fly ash, but could be, if appropriate sample preparation methods were added to the procedures.

For determination of the packing properties of fly ash, we selected an instrument called a Powder Characteristics Tester, also available from Hosokawa Micron International, Inc. Again, we have previously reported extensive aerated and packed porosity data obtained with this instrument and discussed experimental procedures (14, 15). The aerated bulk porosity represents the maximum porosity at which the dust sample can support itself. The packed porosity values appear to be a good indication of the tendency of the fly ash to pack under dust cake conditions, which means that packed porosity might be used to predict pressure drop. While many researchers have discussed cake collapse as a possible result of increased pressure drop, Schmidt and Loffler (16), by looking at porosity as a function of cake depth, quantified the effect. Packed porosity values as low as 31% have been measured for a fairly noncohesive fly ash, reflecting the potential of the dust cake to collapse under increased pressure drop and repeated bag cleaning. The aerated porosity, however, is more indicative of the initial porosity of the dust layer as it originally developed.

Both the tensile strength and aerated or packed porosity measurements appear to be good methods to quantify the cohesive properties of fly ash. A question exists as to whether the tensile strength and porosity measurements are simply different methods of determining the same cohesive characteristic; however, Figure 1 indicates that since there is not a good correlation between tensile strength and aerated or packed porosity, the two

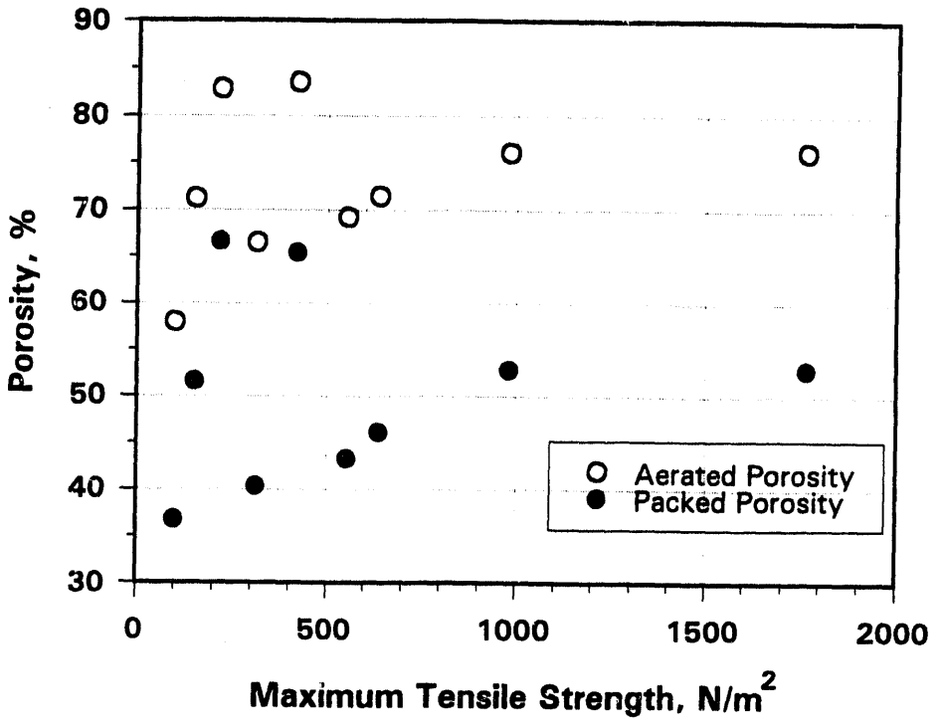

Figure 1. Correlaton between aerated or packed porosity and tensile strength.

measurements provide independent information. Even though these measurements look promising, a consensus needs to be formed to standardize measurements and procedures for determination of cohesive fly ash properties.

– Correlation Between Rapping Reentrainment and Tensile Strength

A pilot study was conducted at the EERC to evaluate enhanced flue gas conditioning methods for improving ESP performance for Wahlco, Inc. and U.S. Department of Energy (DOE) (17, 18). Since one of the mechanisms of performance improvement with conditioning agents was known to be changes in cohesive dust properties, the tensile strengths of conditioned and baseline ESP hopper ash samples were measured with the Cohetester. Tests were conducted with a pilot-scale pulverized coal-fired combustor and a single-wire tubular ESP that had a plate length of 79 in and an inside diameter of 8.3 in. The gas velocity through the ESP was held constant at 5 ft/sec, giving a specific collection area (SCA) of 124 ft^2/1000 acfm. Respirable mass particulate emissions were measured continuously with a TSI model APS 33 laser particle sizer. Respirable mass is defined by the American Council of Governmental and Industrial Hygienists as a weighted sum of particles between 1 and 10 μm with greater weighting given to the smaller particles. Rapping reentrainment was not a primary focus of the study, but rapping emissions data were taken for a variety of conditions since the APS could quantify very short emissions spikes. Respirable mass rapping emissions as a function of maximum tensile strength (i.e., the tensile strength measured at a maximum compaction of 2.5 x 10^4 N/m^2) are shown in Figure 2 for a West Virginia bituminous coal. Tensile strengths were altered by

injecting varying amounts of ammonia and SO_3 as dual conditioning agents into the flue gas upstream of the ESP. The lowest tensile strengths occurred for baseline tests with no conditioning. Note that there was a two-orders-of-magnitude decrease in rapping emissions with an increase in tensile strength. At the higher tensile strengths, there was no measured increase in respirable mass emissions with on-line rapping over the background emissions, even though ash was removed from the plate. This implies that particles in the 1- to 10-μm range were not redispersed as individual particles, but remained as large agglomerates that easily reached the hopper. On the other hand, the data indicate that for low-tensile-strength dusts, particles are readily redispersed as individual particles with rapping. To achieve low emissions with a very-low-tensile-strength dust would require a much larger ESP with more fields. The data indicate that dusts with a tensile strength less than 50 N/m^2 are quite susceptible to particle redispersion and that dusts with a tensile strength of 500 N/m^2 will have minimal fine-particle reentrainment. The data also suggest that no further benefit is seen when the tensile strength is increased beyond 500 N/m^2. Caution must be emphasized that the relative value of the rapping emissions is more important than the absolute value of the emissions, because of the significant differences between a full-scale ESP and the pilot-scale system. The data do show, however, a quantitative relationship between the level of fine-particle rapping reentrainment and fly ash tensile strength and suggest that knowledge of the tensile strength of fly ash might be used to improve ESP performance, either by design changes or by the use of conditioning agents.

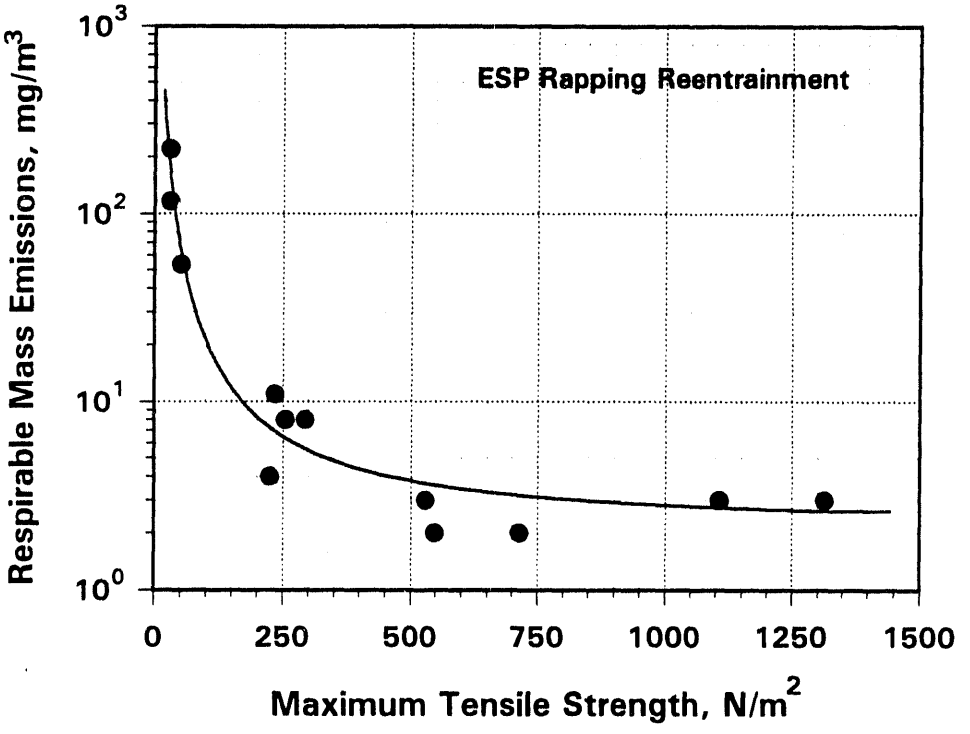

Figure 2. ESP rapping reentrainment of respirable mass particulate emissions as a function of fly ash tensile strength.

– Correlation Between Fabric Filter Emissions and Tensile Strength

Previous research at the EERC investigating methods to improve fabric filter performance by flue gas conditioning has shown that the conditioning process significantly changes the cohesive properties of fly ash (7, 8). In general, the conditioning increases the tensile strength at constant porosity, which indicates that there is an increase in particle-to-particle binding forces. While the evidence is strong that particulate emissions are related to the cohesive characteristics of the dust, a quantitative relationship between emissions and any well-defined cohesive measurement has not previously been developed. In addition to cohesive fly ash properties, fabric filter emissions will depend on particle size, fabric pore size, fabric fiber diameter, bag-cleaning frequency, and face velocity. Therefore, the other variables should be held constant to evaluate particulate emissions as a function of cohesive properties.

A pilot-scale study was recently conducted at the EERC to evaluate the effectiveness of flue gas conditioning in reducing tube sheet pressure drop and fine-particulate emissions from a pulse-jet fabric filter (8, 19). The project was jointly funded by DOE, the Electric Power Research Institute (EPRI), and the Canadian Electrical Association (CEA). The investigation included baseline tests and tests in which ammonia and SO_3 were injected upstream of the baghouse to determine the effect of conditioning on baghouse performance. The primary independent variables included coal type, conditioning agent concentrations, air-to-cloth (A/C) ratio, and fabric type. The main dependent variables were particulate emissions, baghouse pressure drop, and cohesive properties of the fly ash. Results demonstrated significant benefits of using conditioning with a pulse-jet baghouse, including a substantial reduction in particulate emissions and pressure drop (or the ability to operate at a higher A/C ratio without increasing pressure drop or bag-cleaning frequency). The improvements in fabric filter performance correlated strongly with a shift in the tensile strength and with increases in the aerated and packed porosity of the fly ash. Figure 3 provides a quantitative look at the relationship between tensile strength and fine-particle emissions for 100-hour pulse-jet tests with Ryton fabric and a constant A/C ratio of 4 ft/min. Average respirable mass emissions, measured with an APS 33 particle sizer, are plotted as a function of maximum tensile strength. Note that there was a two-orders-of-magnitude decrease in respirable mass particulate emissions as the tensile strength increased from about 100 to 250 N/m^2, and no further decrease in emissions was seen with a further increase in tensile strength. The data indicate that dusts with a maximum tensile strength of less than 100 N/m^2 are more difficult to collect in a fabric filter; therefore, greater care must be taken with fabric selection, face velocity, and cleaning method to ensure a high collection efficiency with low-tensile-strength dusts. These fabric filter emissions results are consistent with the ESP rapping reentrainment results in that dusts with tensile strengths lower than 100 N/m^2 present the greatest collectibility problem. This is not surprising because the level of dust redispersion is likely to contribute to high emissions in fabric filters as well as in ESPs. However, in fabric filters, the pore-bridging ability of the dust will also have an effect on particulate emissions. If the pore-bridging ability of the dust could also be predicted by the dust tensile strength, there would be even stronger evidence that tensile strength is a good indicator of dust collectibility in fabric filters.

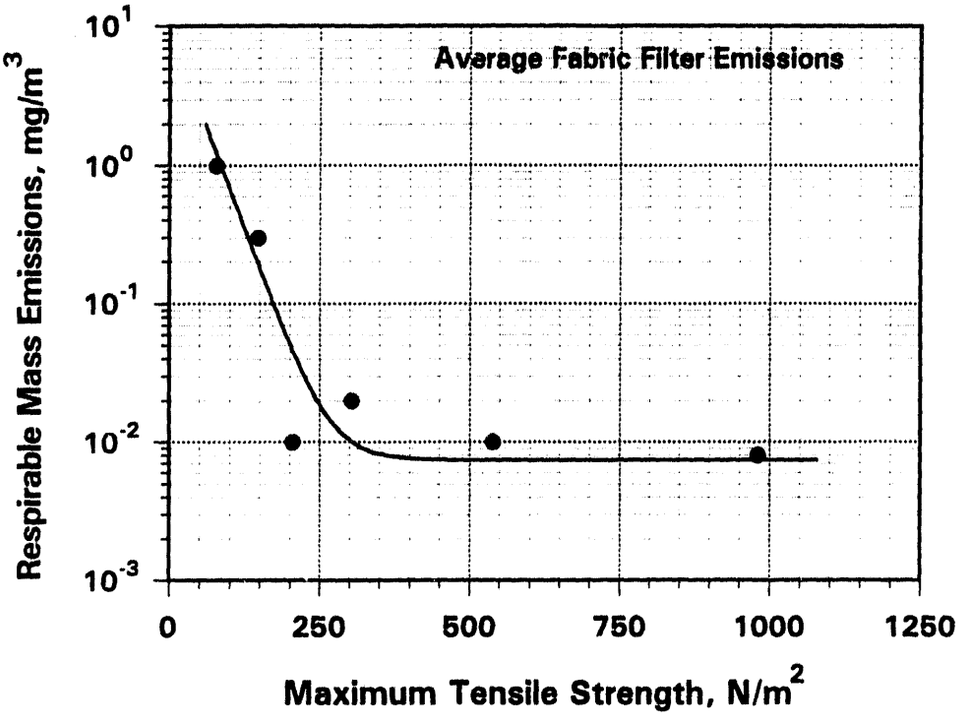

Figure 3. Respirable mass particulate emissions as a function of fly ash tensile strength for 100-hour pulse-jet tests with Ryton fabric at an A/C ratio of 4 ft/min.

We have previously presented results from pore-bridging experiments with a bench-scale system consisting of an 8- x 8-in filter and a dry powder disperser to introduce the fly ash into the carrier gas upstream of the filter (14, 20). Tests were conducted at ambient temperature without added conditioning agents under controlled relative humidities. Dust was introduced at a rate of 1.6 g/min for a period of 35 min, while particulate emissions and pressure drop were recorded as a function of time. Inspection of both the clean and dirty sides of the filters through sight ports gave visual proof of complete pore bridging or the formation of pinholes.

An initial test matrix was conducted at 10% relative humidity with five pore sizes: 300, 150, 75, 40, and 20 μm; four face velocities: 1, 2, 4, and 8 ft/min; and two dust types: baseline and conditioned Monticello fly ash. The filters were precision electroformed nickel sieves, available from Buckbee-Meers, and had square openings. The data from this test matrix showed that conditioning, velocity, and pore size were critical parameters in predicting whether complete pore bridging will occur without reentrainment or pinhole formation. The data appeared to be well behaved in terms of establishing the maximum velocity at which bridging occurs for a given pore size, as shown in Figure 4. Results indicate that the effect of conditioning is to increase the range of pore size and velocities at which good pore bridging will occur. If pore size and velocity are kept below the maximum values shown, excellent collection efficiency should be achieved.

Pore-bridging tests were also conducted with the baseline and conditioned fly ash samples at 50% relative humidity. For the baseline ash, results showed that an increase in relative humidity had very little effect on the maximum pore-bridging velocity. However, the pore-bridging ability of the conditioned ash was greatly improved at 50% relative humidity, as shown in Figure 4. These results are consistent with the tensile strength data. Increasing the relative humidity from 10% to 50% did not increase the tensile strength of the baseline ash but did increase the tensile strength of the conditioned ash. Maximum bridging velocity as a function of maximum tensile strength for the 150-μm pore size is shown in Figure 5. Although only three data points were available, the data indicate that pore-bridging ability is predicted by tensile strength and that low filtration velocities are required to achieve high collection efficiency for dusts with tensile strengths less than 100 N/m^2. The bench-scale pore-bridging data and fabric filter emissions data provide strong evidence that tensile strength is a good predictor of dust collectibility in a fabric filter. The relationships are quantitative in that both emissions and maximum bridging velocity are given as a function of tensile strength. The usefulness of the correlations will depend on whether fabrics can be simulated by screens of exact pore sizes and whether other variables of interest such as porosity, particle size, velocity, cleaning methods, and cleaning frequency can be included in a more general model.

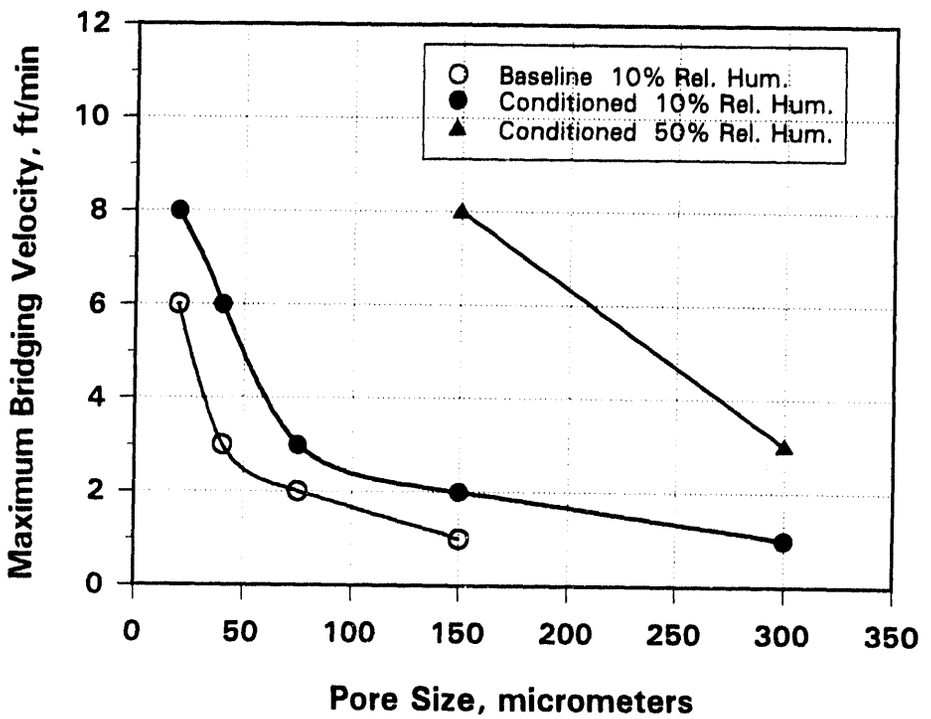

Figure 4. Effect of pore size on maximum pore-bridging velocity for screen tests with baseline and conditioned Monticello fly ash.

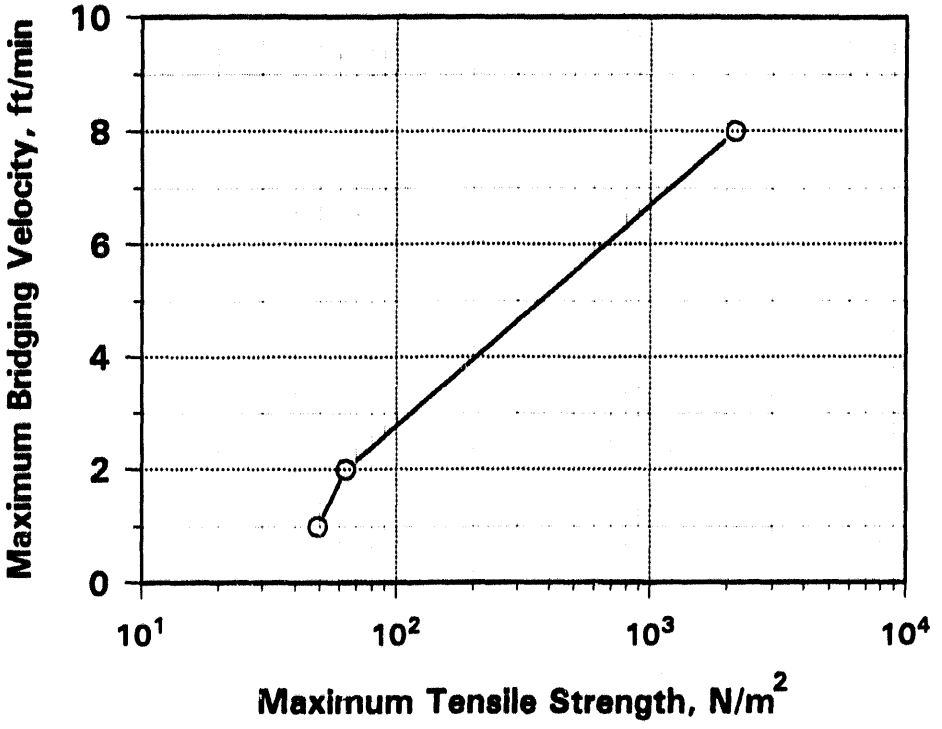

Figure 5. Maximum pore-bridging velocity for 150-μm screen as a function of fly ash tensile strength.

– Correlation Between Fabric Filter Pressure Drop and Packed Porosity

Assuming viscous flow, pressure drop across a fabric filter is given as:

$$\Delta P = K_f V + K_2 W_R V + K_2 C V^2 t/7000 \qquad \text{[Eq. 1]}$$

where ΔP = differential pressure across the baghouse tube sheet (inches of water)
K_f = fabric/dust resistance coefficient (inches of water-min/ft)
V = face velocity or air-to-cloth ratio (ft/min)
K_2 = specific dust cake resistance coefficient (inches of water-ft-min/lb)
W_R = residual dust cake weight (lb/ft^2)
C = dust loading (grains/acf)
t = filtration time between bag cleanings (min)

The first term in Equation 1 accounts for the pressure drop across the fabric. For a new fabric, pressure drop across the fabric alone is generally negligible, but in cases where the dust packs permanently into the interstitial spaces of the fabric, this may be a significant term. The second term in Equation 1 accounts for the pressure-drop contribution from the permanent residual dust cake that exists on the surface of the fabric. In many cases, after long-term operation, this is a significant term. The third term in Equation 1 accounts for the pressure-drop contribution from the dust accumulated on the bags since

the last bag cleaning. K_2 is determined primarily by the fly ash particle-size distribution and the porosity of the dust cake. For accurate prediction of pressure drop, the primary challenge is to predict both K_2 and W_R. As previously stated, both the residual dust cake weight and the porosity of the dust cake will depend on cohesive dust properties. This means that both can probably be predicted from quantitative measurements such as tensile strength or porosity. K_2 values can be reported as an initial value and as the effective value. The initial value is based on the linear part of the ΔP-versus-time curve from the first filtration cycle, starting with new bags. During the first filtration cycle, the ΔP contribution from the first term is negligible, and there is no residual dust cake, so K_2 can be readily obtained from the third term in Equation 1. An effective K_2 value is based on a ΔP that is an average of the difference between the before- and after-cleaning ΔPs. Effective K_2 is higher than the initial K_2 because the bags generally do not clean uniformly, and some of the dust is dispersed and redeposited on the bags after on-line pulsing. Therefore, effective K_2 includes cake release and redispersion in addition to particle size and porosity. The correlations shown in Figure 6 for the 100-hour pulse-jet tests indicate that both initial and effective K_2 can be predicted by the packed porosity of the fly ash. The data are from tests with Ryton fabric at A/C ratios of 4 and 6 ft/min with three different coals. These correlations likely would not be valid, however, if the particle-size distributions varied significantly.

The more complex dependence of K_2 on face velocity and particle size in addition to cohesive properties is shown in Figure 10, which presents K_2 data from bench-scale pore-bridging experiments. The K_2 dependence on velocity is much less significant for the more cohesive conditioned samples than for the baseline samples. The 4.5-μm-mass-median-diameter (MMD) dusts had higher K_2 values, as expected. Pressure-drop models, such as Carman-Kozeny, exhibit an inverse square relationship between K_2 and particle size, which indicates that K_2 for a 4.5-μm dust would be approximately 8 times greater than the K_2 for a 13-μm dust at constant porosity. Typically, a smaller particle size forms a more porous cake, partially offsetting the particle-size effect. Thus, the K_2 values of the 4.5-μm dusts were only from 1.2 to 2.5 times greater than the K_2 values of the 13-μm dusts. In addition, MMD values generally cannot be used in the theoretical Carman-Kozeny model, which is based on monosized particles. For fabric filters with a narrow range in face velocity and filtering dusts of similar particle-size distributions, it appears that packed porosity measurements are good predictors of K_2, as indicated by Figure 6. A more general predictive model for K_2, however, must include particle size and face velocity in addition to packed porosity.

– Summary and Discussion of Preliminary Modeling Efforts

Tensile strength, aerated porosity, and packed porosity measurements are appropriate methods to quantify the cohesive properties of fly ash. Fly ashes with tensile strengths of less than 50 N/m^2 are likely to have significantly greater ESP rapping dispersion of fine particles than fly ashes with tensile strengths greater than 250 N/m^2. Fly ash tensile strength also appears to be a good predictor of fabric filter particulate emissions. Fine-particle emissions from a pulse-jet baghouse with Ryton felted fabric were 100 times greater for a fly ash with a tensile strength less than 100 N/m^2 compared to fly ashes with tensile strengths greater than 250 N/m^2. In direct pore-bridging experiments with monosized openings, tensile strength was found to be an indicator of maximum bridging velocity. In tests with pulse jet-cleaned Ryton bags, packed porosity was a good

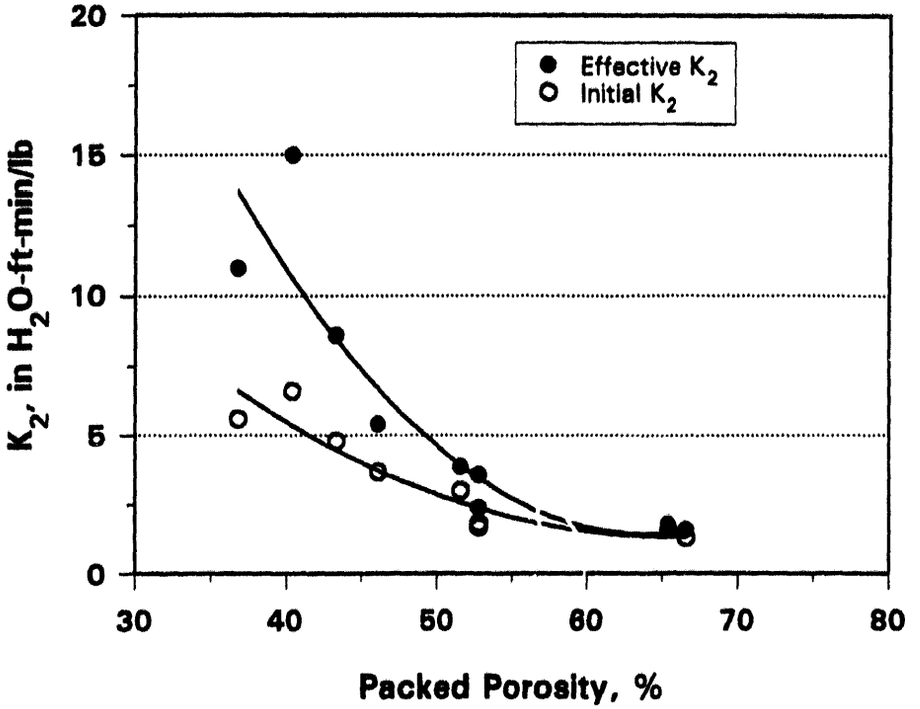

Figure 6. Initial and effective K_2 as a function of packed porosity for 100-hour pulse-jet tests with Ryton fabric at A/C ratios of 4 and 6 ft/min.

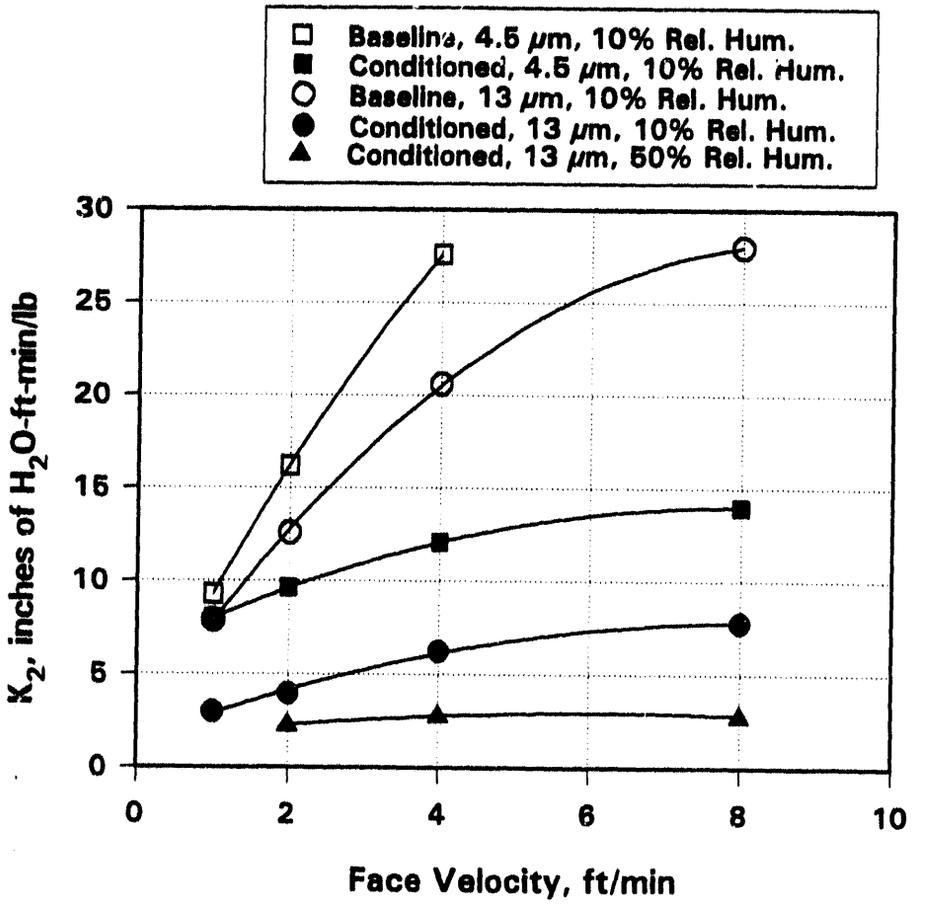

Figure 7. Effect of face velocity on K_2 for screen tests with baseline and conditioned Monticello fly ash.

indicator of initial or effective K_2. Bench-scale tests, however, indicate that particle size and face velocity must also be incorporated into a model to predict pressure drop as a function of dust properties.

● BENCH-SCALE PORE-BRIDGING AND REENTRAINMENT EXPERIMENTS

Last year, the EERC conducted tests with a horizontal reentrainment test system (flow parallel to the ash surface) to determine the threshold velocities at which reentraiment would occur (21). An objective of the horizontal reentrainment tests was to determine the velocity at which reentrainment occurs, relating reentrainment velocity to the cohesive properties of the ash and, ultimately, to the particle-particle binding forces. The particle-particle binding forces can be approximated as follows. Measured tensile strengths of baseline and conditioned fly ash with an MMD of about 13 μm have ranged from 10 N/m^2 to 2000 N/m^2. Assuming monosized 13-μm spherical particles and simple cubic packing (corresponding to a porosity of 47.6%), there would be 590,000 particles in contact in an area of 1 cm^2. This corresponds to an average particle-particle binding force of 1.7×10^{-8} N for a dust with a tensile strength of 10 N/m^2. The actual particle-particle binding force will likely be somewhat higher because the porosity is typically greater than 47.6% and the pore structure will not result in a perfect packing arrangement. The particle-particle binding forces must be overcome by a fluid drag force for particle reentrainment to occur. Applying Stokes' law, the velocity at which the drag force is equivalent to a 1.7×10^{-8} N particle-particle binding force is 25 ft/sec for a 13-μm spherical particle. This velocity is within the range of velocities for which significant reentrainment was observed. The actual conditions at the boundary layer, where the reentrainment occurred, are unknown; however, the Reynolds numbers for flow through the flow gate in the horizontal reentrainment test system were well within the turbulent flow region. The most significant reentrainment occurred somewhat downstream from the gate and may have been influenced by turbulent eddies. Although a laminar sublayer may exist at the dust surface, calculation of the exact drag force on the particles that were reentrained is difficult because the exact location where the particles were initially at rest (relative to the gate orientation) is unknown, and turbulent conditions were present. Nevertheless, the results indicate that fairly high velocities are necessary to produce a Stokes' drag velocity of 25 ft/sec in order to overcome a particle-particle binding force of 1.7×10^{-8} N.

Velocities in the range of 5 to 25 ft/sec are 75 to 375 times greater than the common filtration face velocity of 4 ft/min used with pulse-jet baghouses. For a dust cake porosity of 50%, the actual velocity of the gas through the cake would be twice as great, which is still 37 times less than the minimum velocity at which reentrainment occurred. This implies that particle reentrainment due to viscous drag within the bulk of a dust cake should not occur under normal filtration conditions since the velocities are too low. On the other hand, if velocities are greater than 5 ft/sec, particle reentrainment is expected. Local velocities can greatly exceed 5 ft/sec when pinholes develop in the dust cake. From capillary flow calculations, the velocity through a 100-μm-diameter pinhole can be 100 to 1000 times greater than the face velocity, or 400 to 4000 ft/min (6.7 to 67 ft/sec) for a typical face velocity of 4 ft/min. Therefore, once pinholes form beyond a critical diameter, it is difficult to bridge them again because of the potential for reentrainment along the edges. After bag cleaning, many of the larger pores are opened, which can also result in localized high velocities. These pores must be bridged quickly for high particulate-removal efficiency. Therefore, dusts with superior pore-bridging ability will obviously be collected with higher efficiencies, and if pore-bridging ability (or resistance to

reentrainment) can be predicted from cohesive measurements, then collection efficiency is also predicted from these measurements.

Since the horizontal reentrainment tests indicated reentrainment will occur only at much higher velocities than are typically found in conventional filtration (except in pinholes), a different type of reentrainment experiment is being conducted this year. The procedure involves the use of the electroformed sieves that were used in the previous pore-bridging experiments. However, ash is fed for only a short interval at a velocity of 2 ft/min so that dust accumulates only along the edges of the openings in the screens. During this interval, particulate emissions are high because bridging of the openings has not occurred yet. The dust feed is then stopped and the velocity is reduced to 1 ft/min while particulate emissions decrease to background levels. The velocity is then increased back to 2 ft/min, which typically results in only a slight increase in emissions. Then the velocity is increased to 4, 8, and 16 ft/min while emissions are monitored. Results from these tests, shown in Figures 8-18, indicate that significant reentrainment spikes occur when the velocity is increased beyond 2 ft/min. This reentrainment occurs at velocities far below the 5-ft/sec (300-ft/min) threshold reentrainment velocity seen with the horizontal reentrainment test system. Since the reentrainment must occur as a result of fluid drag overcoming particle-particle binding forces, and the particle-particle binding forces are expected to be similar, the reentrainment geometry must be different. To bridge the 150-μm openings in the screen, 10 to 15 particle layers are required. Therefore, the particle deposit structure prior to bridging must consist of long chains of particles that are loosely attached to the edges of the screen openings. These structures protruding from the screen edges evidently can be reentrained at much lower velocities than individual particles. The exact nature of the reentrainment that occurs would be more obvious if photographs of the deposit structure were available before and after the reentrainment. Attempts to produce photographic evidence of the reentrainment are discussed later.

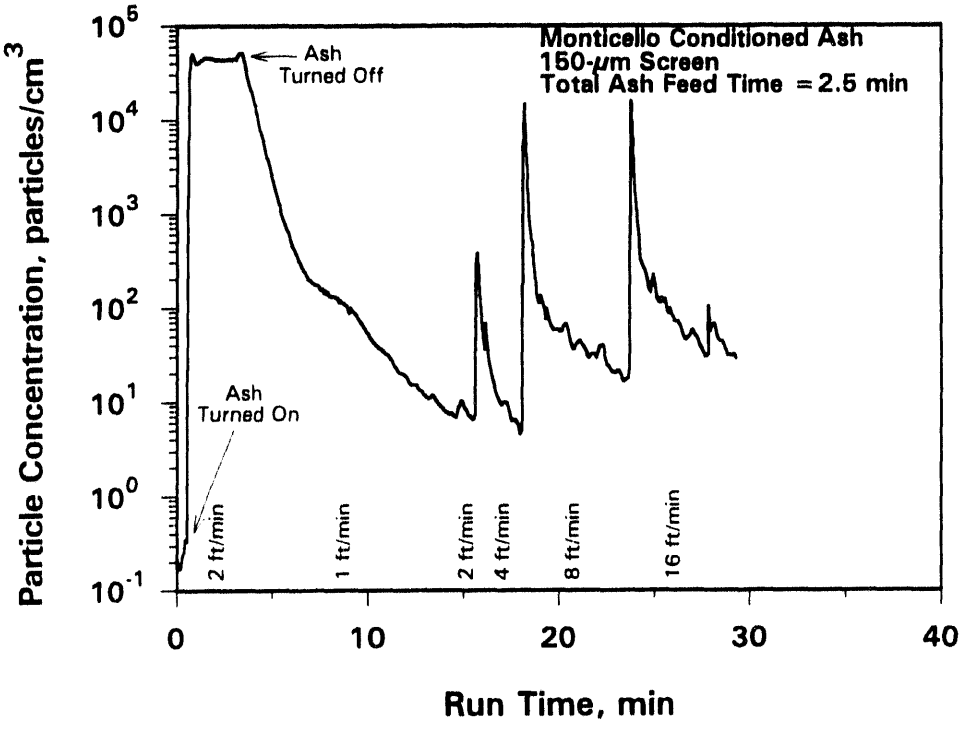

Figure 8. Particle reentrainment from a 150-μm screen measured with a condensation particle counter with an initial ash feed time of 2.5 minutes.

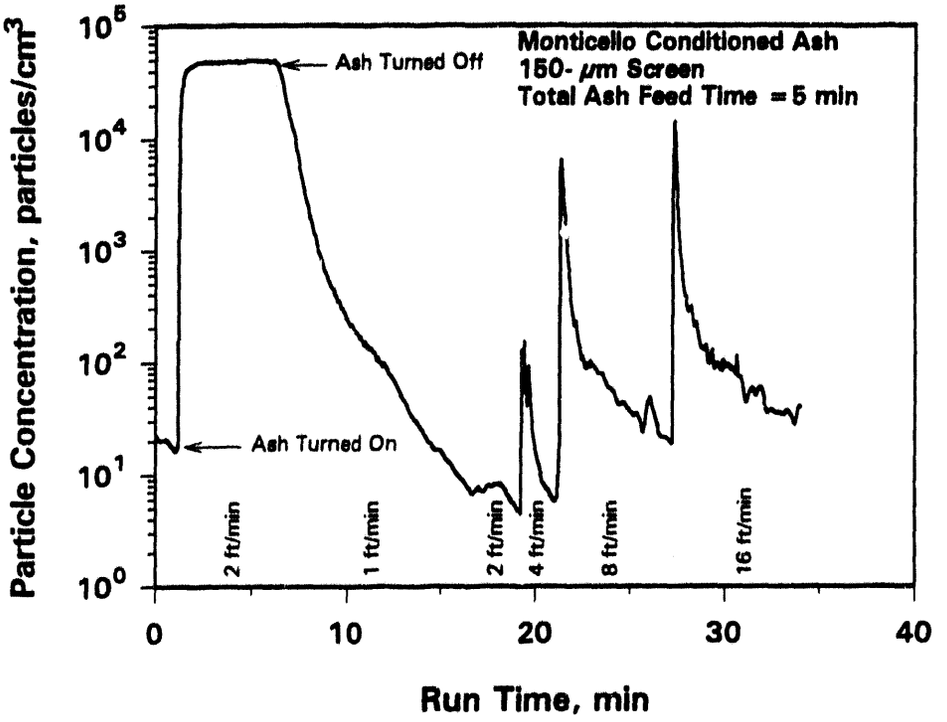

Figure 9. Particle reentrainment from a 150-μm screen measured with a condensation particle counter with an initial ash feed time of 5 minutes.

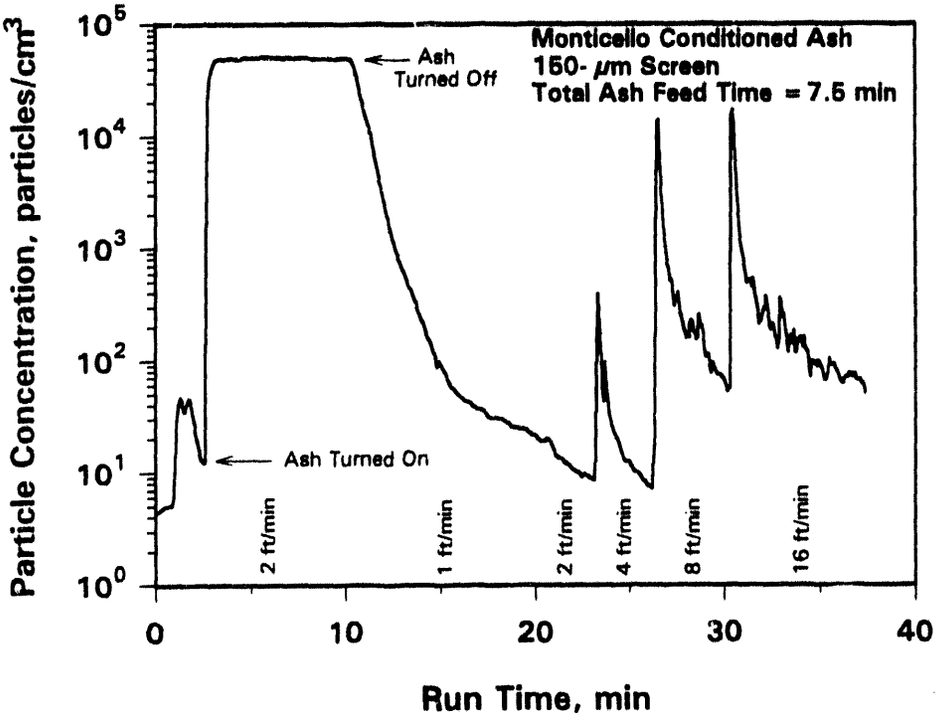

Figure 10. Particle reentrainment from a 150-μm screen measured with a condensation particle counter with an initial ash feed time of 7.5 minutes.

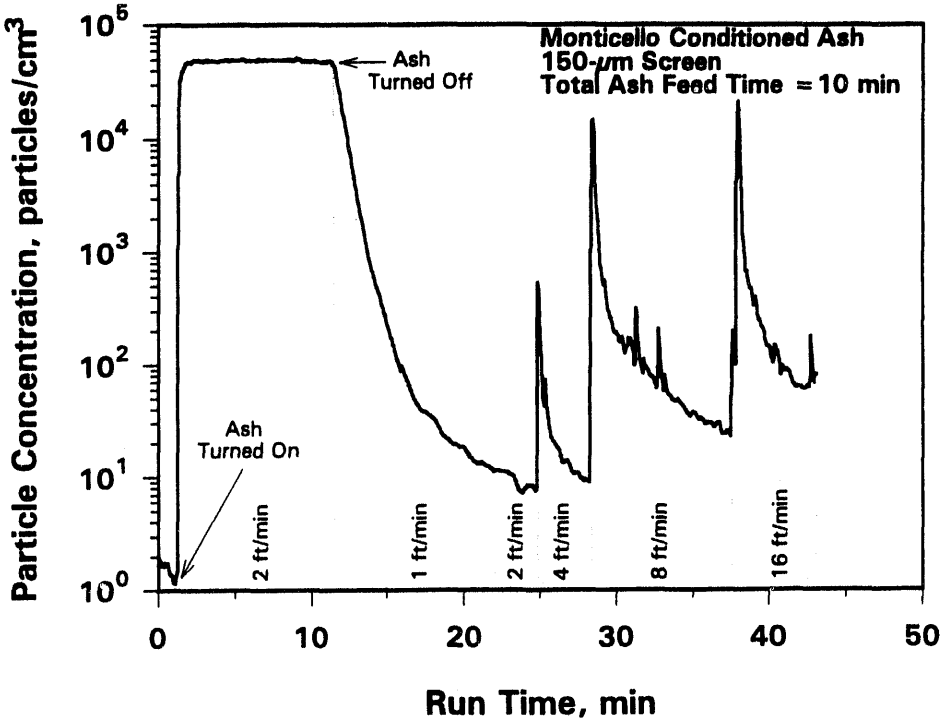

Figure 11. Particle reentrainment from a 150-μm screen measured with a condensation particle counter with an initial ash feed time of 10 minutes.

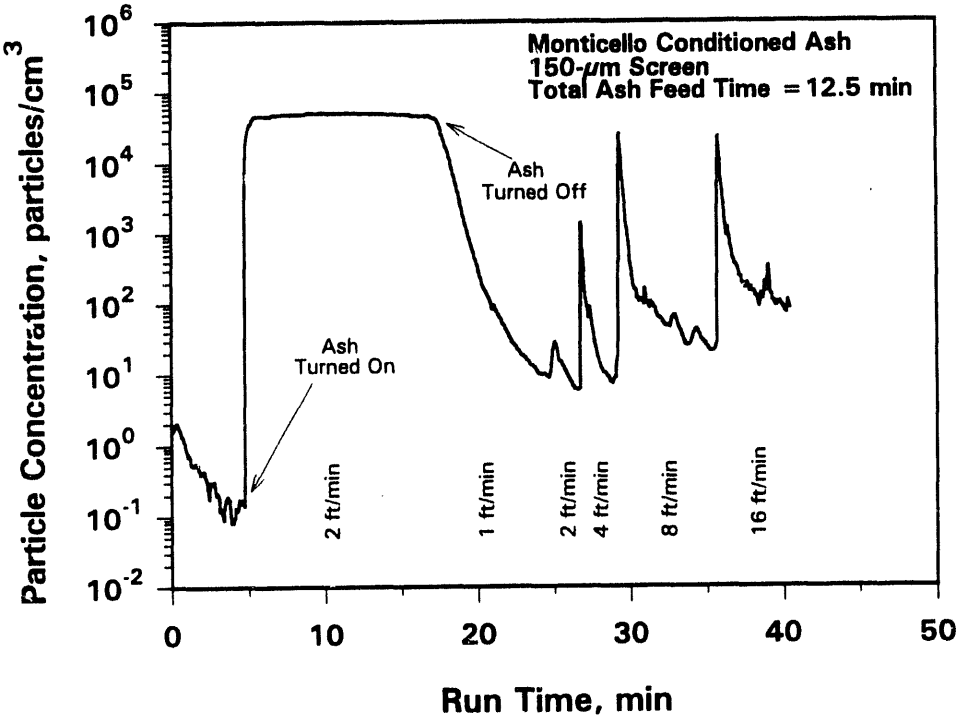

Figure 12. Particle reentrainment of a 150-μm screen measured with a condensation particle counter with an initial ash feed time of 12.5 minutes.

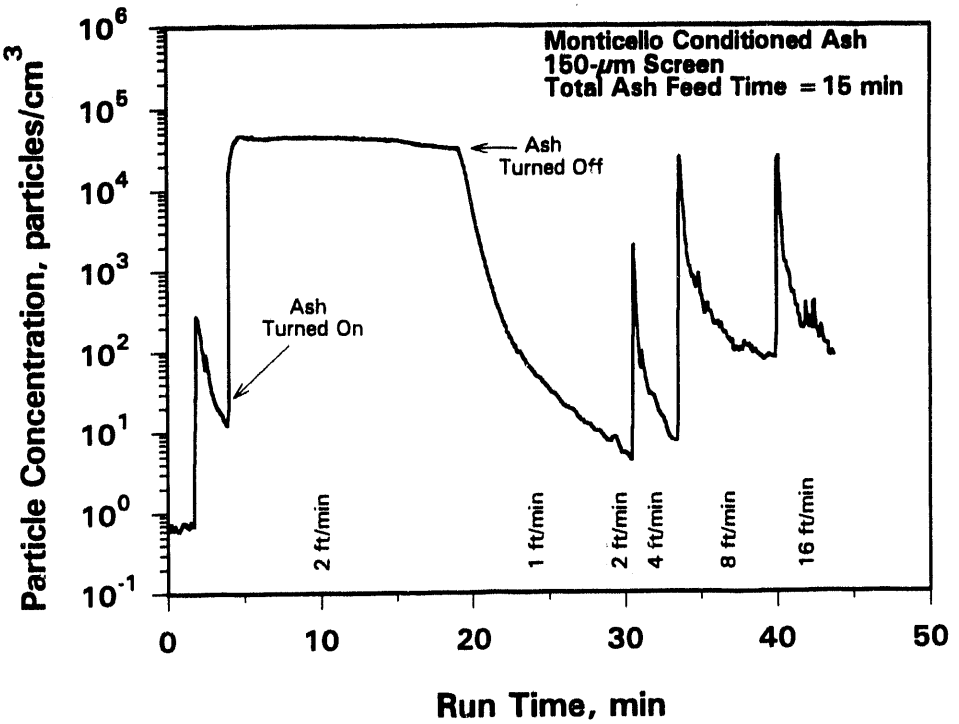

Figure 13. Particle reentrainment from a 150-μm screen measured with a condensation particle counter with an initial ash feed time of 15 minutes.

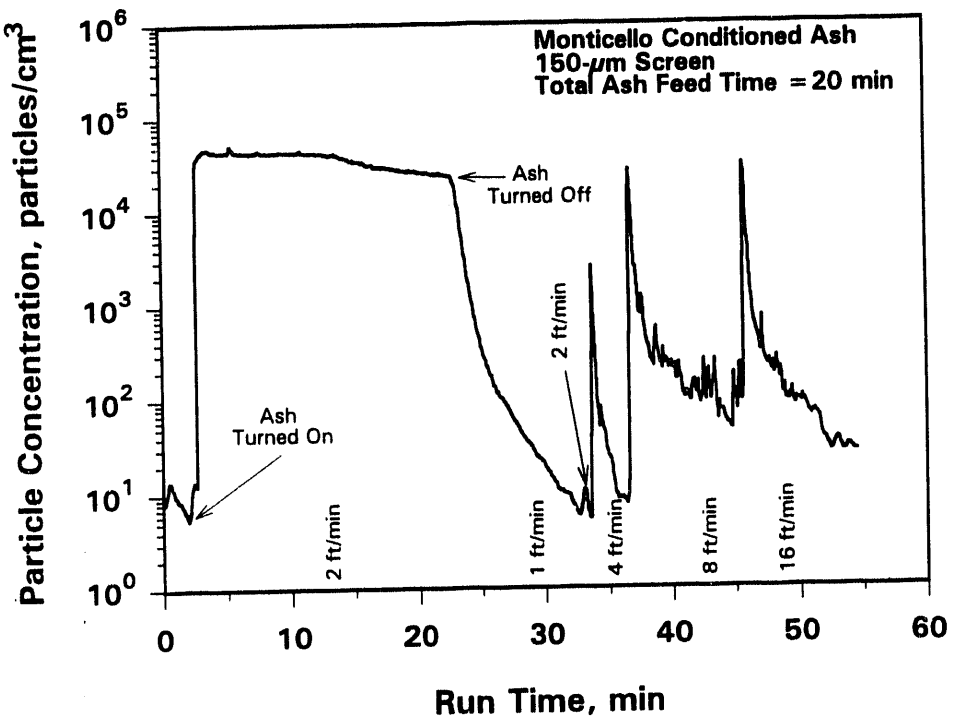

Figure 14. Particle reentrainment from a 150-μm screen measured with a condensation particle counter with an initial ash feed time of 20 minutes.

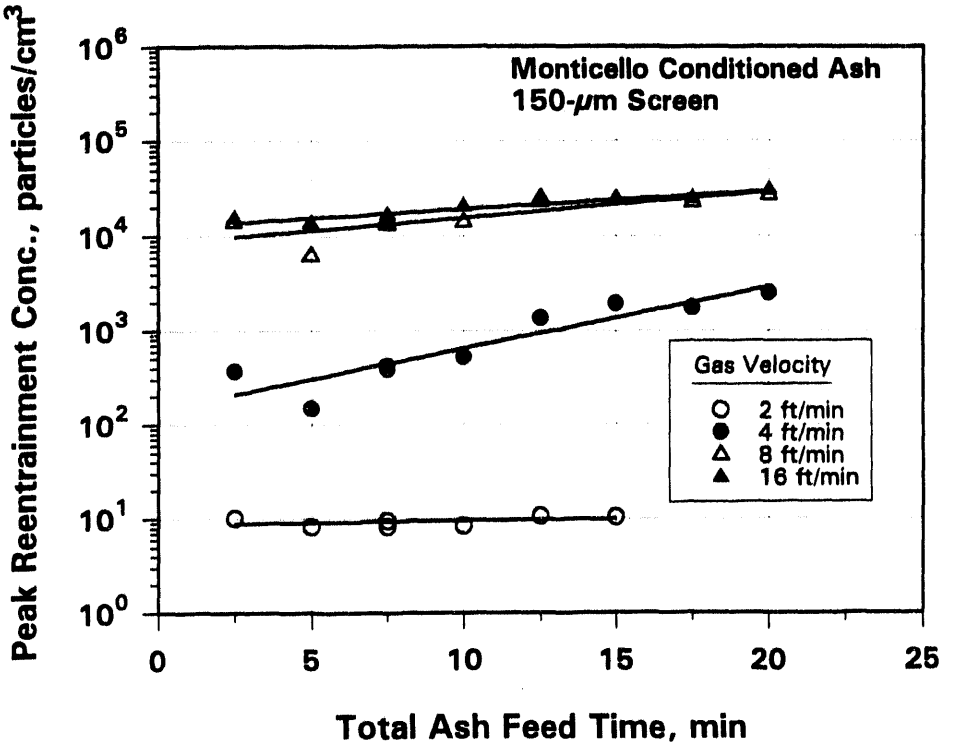

Figure 15. Summary of peak reentrainment concentration measured with a condensation particle counter as a function of initial ash feed time for conditioned Monticello fly ash and a 150-μm screen.

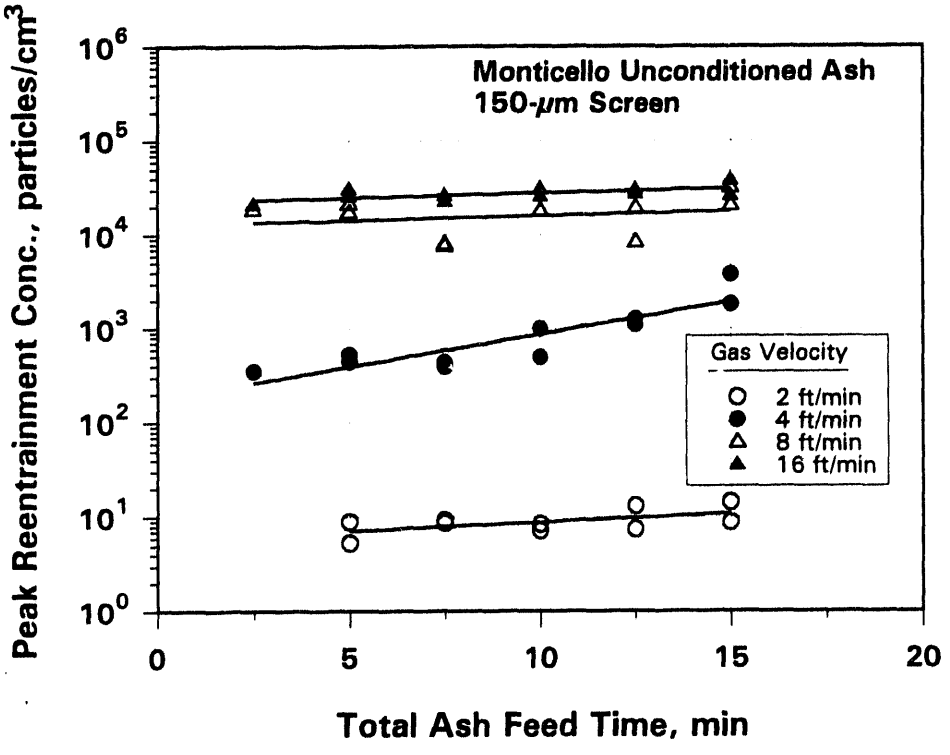

Figure 16. Summary of peak reentrainment concentration measured with a condensation particle counter as a function of initial ash feed time for baseline (unconditioned) Monticello fly ash and a 150-μm screen.

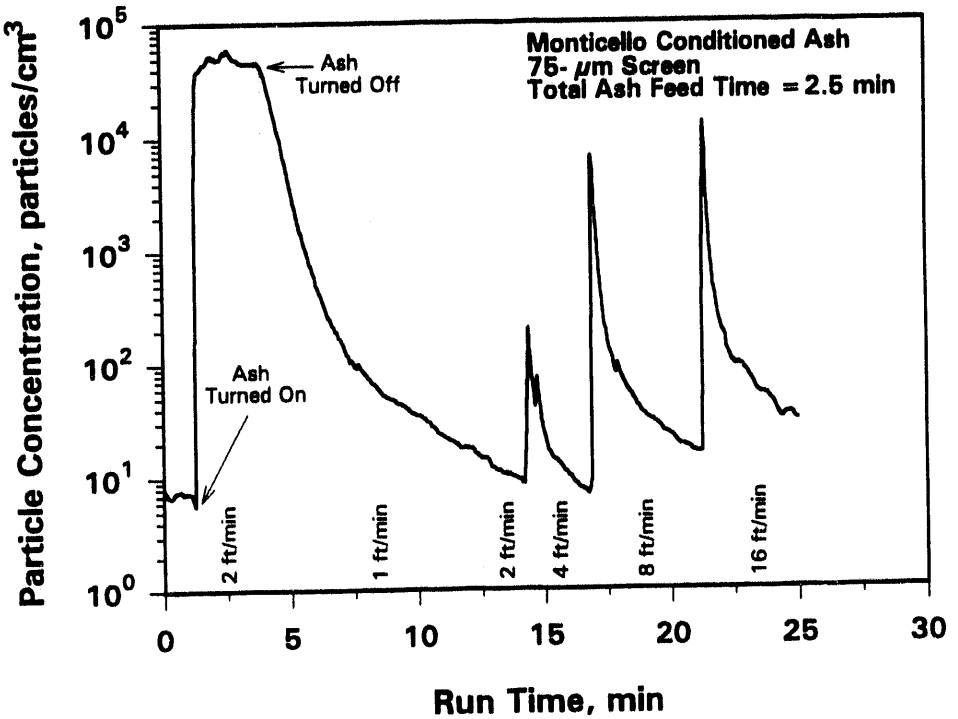

Figure 17. Particle reentrainment from a 75-μm screen measured with a condensation particle counter with an initial ash feed time of 2.5 minues.

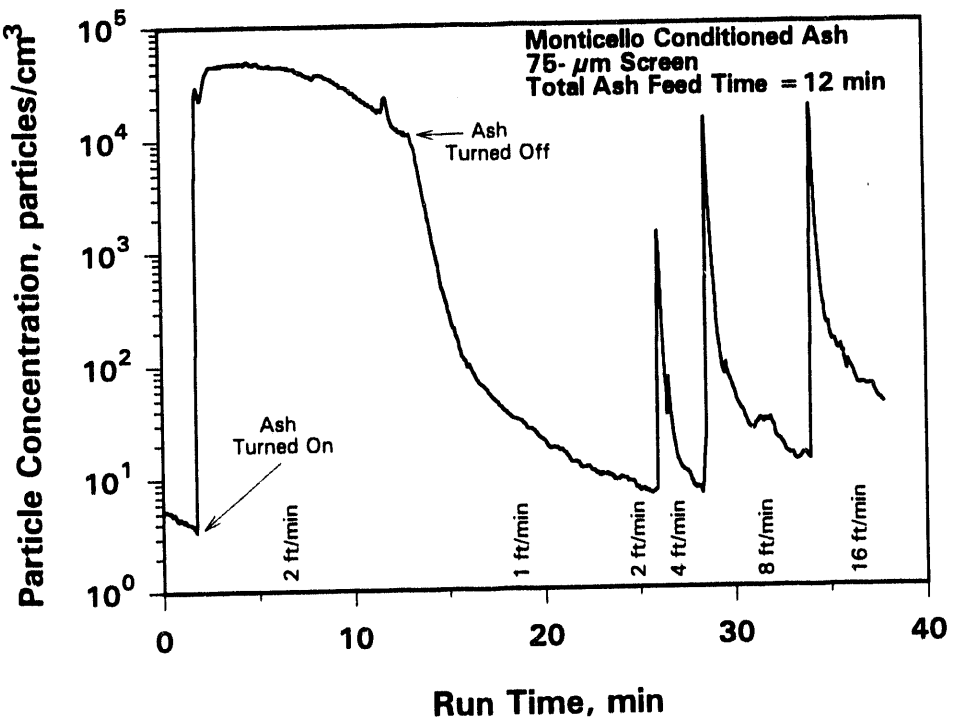

Figure 18. Particle reentrainment from a 75-μm screen measured with a condensation particle counter with an initial ash feed time of 12 minutes.

One of the variables of interest is the relationship between the length of time of initial dust feed and the level of emissions. Similar reentrainment tests were conducted with initial ash feed times ranging from 2.5 to 20 minutes. At 20 minutes, complete pore bridging still had not occurred. Results from a series of these tests, shown in Figures 15 and 16 indicate that the concentrations of the reentrainment spikes at 4, 8, and 16 ft/min were somewhat affected by the initial feed time but perhaps not to the extent expected. Velocity, however, appears to be the most critical parameter affecting the level of reentrainment. In general, the reentrainment at 2 ft/min was just detectable above the background. This is not surprising since the particles were initially collected at a face velocity of 2 ft/min. If the particles were retained at that velocity during initial collection, they would not be expected to reentrain after the velocity is reduced to 1 ft/min and then increased again to 2 ft/min. However, when the velocity was increased to 4 ft/min, noticeable reentrainment occurred over the entire range of initial ash feed times. When the velocity was increased to 8 ft/min, the reentrainment spike was a factor of 10 times greater than at 4 ft/min. This reentrainment is in addition to the reentrainment at 4 ft/min, since the tests were conducted in sequence without additional ash feed between the increases in velocity. At 16 ft/min, the reentrainment spike was about the same as at 8 ft/min, but this also represents additional reentrainment that did not occur at 8 ft/min. Figures 17 and 18 indicate that similar levels of reentrainment were seen when the screen size was reduced to 75 μm. Evidently multiple particle chains are still formed during the initial bridging process and these structures are very susceptible to reentrainment.

Initial attempts to photograph the pore-bridging structure indicate that the particles initially form chainlike structures that eventually meet to form a bridge over the 150-μm openings. Further tests are being conducted in which we are attempting to photograph the structure of the deposit before each increase in velocity to determine the type of structure that is reentrained, but these tests have not been completed yet. Occasionally, after complete bridging (depending on velocity and dust tensile strength), an entire bridge will break loose. This results in a higher-velocity pinhole that is then more difficult to bridge again since the level of reentrainment is greater at the higher velocity.

These reentrainment tests indicate that face velocity is one of the most important parameters affecting pore-bridging ability and reentrainment potential. Therefore, future modeling efforts to relate emissions to cohesive properties should also attempt to incorporate velocity. We expect the general trend that was demonstrated in Figure 3 to hold true, showing the strong dependence of emissions on tensile strength. However, at higher velocities, a much greater tensile strength may be required to achieve the same level of fine particulate collection efficiency that can be achieved at lower velocities. Therefore, a model that can adequately predict emissions from both tensile strength and velocity data is needed.

References

1. White, H.J. *Industrial Electrostatic Precipitation*; Addison-Wesley: Reading, MA, 1963.

2. Dismukes, E.B. "Conditioning of Fly Ash with Sulfur Trioxide and Ammonia," EPA-600/2-75-015, Aug. 1975.

3. Spencer, H.W. III. "Rapping Reentrainment in a Nearly Full-Scale Pilot Electrostatic Precipitator," EPA-600/2-76-140, May 1976.

4. Billings, C.; Wilder, J. *Handbook of Fabric Filter Technology, Volume I: Fabric Filter Systems Study*; GCA Corporation: Bedford, MA, 1970.

5. Dennis, R.; et al. "Filtration Model for Coal Fly Ash with Glass Fabrics," EPA-600/7-77-084, Aug. 1977.

6. Bush, P.V.; Snyder, T.; Chang, R. "Determination of Baghouse Performance from Coal and Ash Properties: Parts I and II," *Journal of the Air and Waste Management Association* **1989**, *39* (2, 3).

7. Laudal, D.L.; Miller, S.J. "Flue Gas Conditioning for Improved Baghouse Performance," *In* Proceedings of the Sixth Symposium on the Transfer and Utilization of Particulate Control Technology; EPRI CS-4918, Nov. 1986, Vol. 3, p 14-1.

8. Miller, S.J.; Laudal, D.L; Chang, R.L. "Flue Gas Conditioning for Improving Pulse-Jet Baghouse Performance," *In* Proceedings of the Ninth Particulate Control Symposium; EPRI TR-100471, April 1992, Vol. 2, p 12-1.

9. Pohl, F.G. "A Novel Ring Shear Device for the Purpose of Classification of Fine Powders," Presented at the 17th Annual Meeting of the Fine Particle Society, San Francisco, CA, July 1986.

10. Pontius, D.H. "Electrostatic Reentrainment and Dispersion of Particles and Agglomerates," *In* Proceedings of the Fourth International Conference on Electrostatic Precipitation; Li, R., Ed.; Beijing, China, 1990.

11. Ashton, M.D.; Farley, R.; Valentin, F.H.H. "An Improved Apparatus for Measuring the Tensile Strength of Powders," *Journal of Scientific Instruments* **1964**, *41*, 763-765.

12. Yokoyama, T.; Fujii, K. "Measurement of the Tensile Strength of a Powder Bed by a Swing Method Measuring Instrument," *Powder Technology* **1982**, *32*, 55-62.

13. Weber, G.F.; Miller, S.J.; Laudal, D.L. "Flue Gas Cleanup," Annual Technical Project Report for the Period July 1, 1989, through June 30, 1990; DE-FC21-86MC10637, EERC publication Grand Forks, ND, Oct. 1990.

14. Weber, G.F.; Miller, S.J.; Laudal, D.L.; Heidt, M.K. "Flue Gas Cleanup," Semiannual Technical Progress Report for the Period January 1, 1991, through June 30, 1991; DE-FC21-86MC10637, EERC publication Grand Forks, ND, Aug. 1991.

15. Miller, S.J. "Flue Gas Conditioning for Fabric Filter Performance Improvement," Final Project Report; DE-AC22-88PC88866, EERC publication Grand Forks, ND, Dec. 1989.

16. Schmidt, E.; Loffler, F. "The Analysis of Dust Cake Structures," *Part. Syst. Charact.* **1991**, *8*, 105-109.

17. Miller, S.J.; Laudal, D.L. "Enhanced Flue Gas Conditioning Study, Final Project Report," EERC publication, Grand Forks, ND, Nov. 1991.

18. Krigmont, H.; Coe, E.; Miller, S.J.; Laudal, D.L. "Enhanced ESP Fine-Particle Control by Flue Gas Conditioning," *In* Proceedings of the Ninth Particulate Control Symposium; EPRI TR-100471, April 1992, Vol. 1, p 4-1.

19. Miller, S.J.; Laudal, D.L. "Pulse-Jet Baghouse Performance Improvement with Flue Gas Conditioning," EERC publication, Grand Forks, ND, Oct. 1992.

20. Miller, S.J.; Heidt, M.K.; Laudal, D.L,; Weber, G.F. "Flue Gas Cleanup," Semiannual Technical Progress Report for the Period July 1, 1991, through December 31, 1991; DE-FC21-86MC10637, EERC publication Grand Forks, ND, Jan. 1992.

21. Miller, S.J.; Heidt, M.K.; Laudal, D.L.; Weber, G.F. "Flue Gas Cleanup," Semiannual Technical Progress Report for the Period January 1, 1992, through June 30, 1992; DE-FC21-86MC10637, EERC publication Grand Forks, ND, July 1992.

DATE

FILMED

5/2/94

END